LOCATION OF CHEMICALLY MODIFIED LYSINE 41 IN THE STRUCTURE OF BACTERIORHODOPSIN BY NEUTRON DIFFRACTION

F. SEIFF, I. WALLAT, J. WESTERHAUSEN, AND M. P. HEYN
Biophysics Group, Department of Physics, Freie Universität, Berlin, Arnimallee 14, D-1000 Berlin 33, West Germany

ABSTRACT Purple membranes were prepared in which bacteriorhodopsin was labeled at lysine 41 with phenylisothiocyanate (PITC) and with perdeuterated PITC. The in-plane position of this small label containing only five deuterons was determined from the differences between the neutron diffraction intensities of the two samples. At 8.7-Å resolution the Fourier difference map revealed a well-defined site between helices 3 and 4. This position was confirmed by a refinement procedure in reciprocal space. Model calculations showed that the observed difference density had the right amplitude for the label. Thus it is possible to locate a small group in a large protein structure by replacing as few as five hydrogens by deuterium. The observed location of PITC restricts the number of possibilities for the assignment of helix *B* in the sequence (to which lysine 41 is attached) to one of the seven helices of the structure. Taking into account the size of the label and the length of the lysine side chain our result excludes helices 1, 2, and 7 as candidates for *B*.

INTRODUCTION

The light-driven proton pump bacteriorhodopsin is one of the best characterized membrane proteins (Stoeckenius and Bogomolni, 1982). Apart from the light-dependent steps involving the chromophore retinal, bacteriorhodopsin has much in common with the large class of proton-translocating membrane proteins. The goal of much of the research in this area is to uncover the mechanism of proton translocation in molecular detail. Three-dimensional structural information is a prerequisite for formulating hypotheses concerning the pumping mechanism. In the case of bacteriorhodopsin, structural work is facilitated by the availability of purple membranes, natural two-dimensional hexagonal lattices of bacteriorhodopsin. On the basis of the amino acid sequence (Ovchinnikov et al., 1979; Khorana et al., 1979), proteolytic digestion and diffraction experiments, a model emerged in which the peptide sequence of bacteriorhodopsin traverses the membrane seven times in the form of alpha helices (Henderson, 1975; Unwin and Henderson, 1975; Hayward and Stroud, 1981; Henderson and Unwin, 1975). There are 7! = 5,040 ways of assigning the seven helical segments in the sequence (labeled *A* to *G*) to the seven helices in the structure (labeled 1 to 7, see Fig. 6). This assignment problem remains to be solved (Engelman et al., 1980; Agard and Stroud, 1982). So far a number of partially contradictory results have been reported. Using x-ray and electron diffraction it was concluded that helix *G* should be identified with helix 2 (Wallace and Henderson, 1982). Helix 1 was excluded as candidate for *G* from electron diffraction experiments with purple membranes in which helix *G* was labeled with a heavy atom (Katre et al., 1984). Model calculations based on neutron diffraction experiments with bacteriorhodopsin that was selectively deuterated in a particular class of amino acids led to the conclusion that helices *F* and *G* should be placed at positions 3 and 4, respectively (Trewhella et al., 1983). In this previous neutron diffraction work, specifically deuterated amino acids were added to the bacterial growth medium and were incorporated biosynthetically (Trewhella et al., 1983; Engelman and Zaccai, 1980). A disadvantage of this procedure is that the label will not appear in a unique helix, but will be spread over several helices. Thus in the case of deuterated valine (Engelman and Zaccai, 1980), seven labeled valines are expected to occur in helix *F*, four in *G*, three in *D*, two in *E*, and one each in *A*, *B*, and *C*. A more direct approach to the helix assignment problem using neutron diffraction is to chemically modify a single amino acid in the sequence with a small label that will necessarily contain only a few deuterons. From the differences in neutron diffraction intensities between samples with protonated and deuterated label, the labeling site can be determined. The uncertainty in the assignment of the helix to which the labeled amino acid is attached will be determined by the size of the label and the length of the amino acid side chain. The method is of course limited by the availability of suitable reacting groups in the amino acid side chains and by the necessity of labeling a unique site. Here this novel approach was applied for the first time. Lysine 41 of helix *B* was labeled with phenylisothiocyanate (PITC) according to a recently developed procedure (Sigrist et al., 1984). Only lysine 41 reacts with the label at a stoichiometry of

close to 1:1 and the label resides in a hydrophobic region of the membrane (Sigrist et al., 1984). PITC contains five protons in its phenyl ring (see Fig. 1). Applying the Fourier difference method to the neutron diffraction intensities for purple membranes labeled with PITC and perdeuterated PITC, a well-defined site was obtained. The position of the label was further refined in reciprocal space. The coordinates obtained in the Fourier difference synthesis served as input starting-values in the refinement procedure. The resulting "best" Fourier difference map showed a peak at very nearly the same position with reduced amplitudes in the rest of the map. Model calculations were performed to prove that the observed density in the Fourier difference map at the site of the label had the amplitude expected for a label of this strength. These calculations showed good agreement between observed and predicted Fourier difference coefficients.

Our result narrows down the number of possibilities for the location of helix *B* to which lysine 41 is attached (Stoeckenius and Bogomolni, 1982; Engelman et al., 1980). We expect that the helix assignment problem can be solved completely with a few more labels of this kind.

MATERIALS AND METHODS

Materials

PITC and deuterated aniline were purchased from Merck (Darmstadt, Federal Republic of Germany). *Halobacterium halobium* strain S9 was grown according to standard procedures (Oesterhelt and Stoeckenius, 1974).

Synthesis of D_5-PITC

D_5-PITC (Fig. 1) was synthesized according to standard procedures (Gattermann-Wieland, 1982). 5 g deuterated aniline ($C_6D_5NH_2$) was boiled for 3 h under backflow together with 6.5 g CS_2, 6.0 g ethanol, and 1.25 g KOH. After distilling off CS_2 and ethanol, water was added to the residue. White crystals of diphenylthiourea formed, which were washed and dried. 3 g diphenylthiourea were added to 12 ml HCl (ρ = 1.8 g/cm^3) and distilled. The distillate was mixed with an equal volume of water and extracted with ether. After drying over $CaCl_2$, the ether was removed in a rotation evaporator and the residue was distilled. The fraction having its boiling point in the range 218–221°C (at 1 atm pressure) was identified as PITC by infrared- and ultraviolet absorption spectroscopy (Fig. 2). The yield was 1.3 g. The ^{1}H-NMR spectrum of D_5-PITC showed no signal, indicating the absence of protons.

Labeling of Bacteriorhodopsin with PITC and D_5-PITC

Purple membranes were labeled according to the protocol of Sigrist et al. (1984). Batches of 52 mg bacteriorhodopsin in 10 ml phosphate buffer (pH 7, 25 mM) were reacted with a 880-fold molar excess of PITC (in ethanol) for 30 min in the dark at 40°C under continuous stirring. The labeled purple membranes were dialyzed for 6 h against 5 l phosphate buffer (pH 7, 10 mM) containing 5 mM cysteine and 0.02% NaN_3 at 20°C. This dialysis procedure was repeated nine times to remove all of the excess label. The decrease in the amount of noncovalently bound label remaining was monitored using the UV absorbance of PITC (see Fig. 2). To remove cysteine the suspension was dialyzed three times against 5 l water, pH 7.0, containing 0.02% NaN_3 (6 h, 20°C). To get enough material for the neutron diffraction experiments, the whole procedure was repeated four times each with PITC and D_5-PITC.

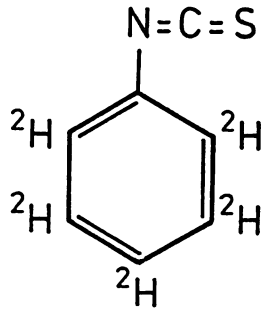

FIGURE 1 Chemical structure of D_5-phenylisothiocyanate.

Characterization of PITC-labeled Purple Membranes

Fig. 3 shows the absorption spectra of purple membranes before (*b*) and after (*a*) labeling with PITC. The spectra were obtained with a Shimadzu 240-UV spectrophotometer (Shimadzu Corp., Kyoto, Japan). The ratio of absorbance at 280 and 570 nm was 1.7 before and ~1.9 after labeling. This corresponds to an estimated loss of retinal of ~10%. Traces of yellow retinal were indeed observed in the first dialysis bag. The x-ray diffraction pattern of these modified membranes shows the normal lattice with slightly broader diffraction maxima. Both the PITC and D_5-PITC samples had the same amount of retinal loss and showed identical x-ray patterns.

Neutron Diffraction Experiments

Sample preparation and experimental conditions were as described in detail elsewhere (Seiff et al., 1985). For each sample, 150 mg of bacteriorhodopsin was applied to 10 quartz slides. For both samples the full width at half height of the mosaic spread was 17°, indicating good orientation. Data collection times were 49 h for the PITC sample and 55 h for the D_5-PITC sample. The data were collected at room temperature and 50% relative humidity in the dark-adapted state of bacteriorhodopsin. The neutron diffraction data were collected on the D-16 diffractometer of the High Flux Reactor (Institute Laue-Langevin, Grenoble).

RESULTS

Fig. 4 shows the raw intensity data from the position-sensitive detector for PITC-labeled purple membranes [(*a*) undeuterated; (*b*) deuterated]. The intensities could be indexed on a hexagonal lattice of unit cell dimension 63 Å. In Fig. 4, the reflection indices (*h*, *k*) are indicated

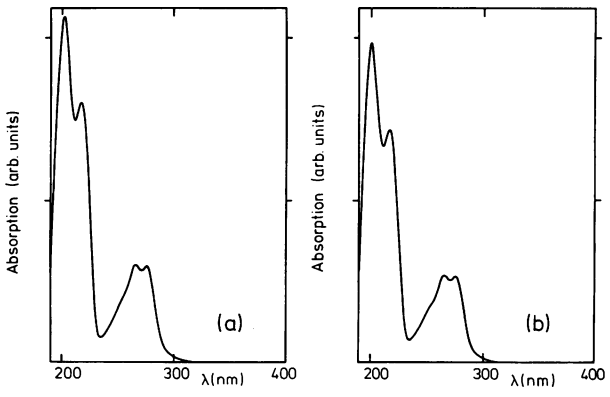

FIGURE 2 Absorption spectra of PITC (*a*) and D_5-PITC (*b*).

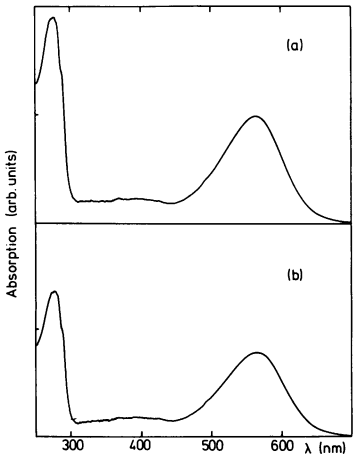

FIGURE 3 Absorption spectra of suspensions of light-adapted purple membranes. (*a*) After reaction with PITC. (*b*) Before reaction with PITC.

above each peak. (7,0) was the highest reflection observed. The (3,0), (3,3), (4,4), and (6,0) reflections are missing. Since only five protons are replaced by deuterons, the intensity differences between Fig. 4 *a* and *b* are expected to be small. Clear changes can nevertheless be observed, for instance in the (4,0) reflection. The background due to an identical stack of 10 quartz slides was measured but shown to be negligible. The background due to the incoherent scattering of the samples was subtracted and the integrated intensities were corrected by a Lorentz factor of $\sqrt{h^2 + hk + k^2}$, which is appropriate for a well oriented sample with a mosaic spread of 17° (full width) (Wallace and Henderson, 1982). The mosaic spread was identical in the undeuterated and deuterated samples, so that both

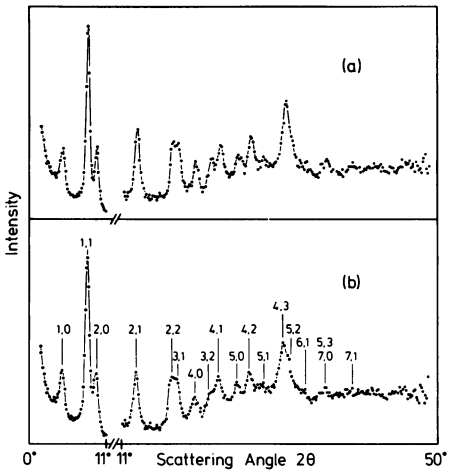

FIGURE 4 Neutron diffraction intensities of oriented purple membranes as a function of the detector angle 2θ. Starting with the (2,1) reflection, the vertical scale has been expanded by a factor of 2.5. (*a*) Labeled with PITC. (*b*) Labeled with D_5-PITC. Shown are the outputs of the position sensitive detector before application of corrections. The vertical lines in *b* labeled with the indices (h, k) indicate the positions of the reflections for a hexagonal lattice with unit cell dimension of 63 Å.

data sets were corrected by the same Lorentz factor. The absorption and projection corrections were proven negligible (Jubb et al., 1984). Since the change in total scattering power of the unit cell due to the replacement of five protons by five deuterons is very small, the structure factors were scaled in such a way that the sum of the intensities of the undeuterated and deuterated samples became equal (Blundell and Johnson, 1976). Before scaling, the two sums differed only by ~10%. The values of the squares of the structure factor moduli for the undeuterated (F_H^2) and deuterated (F_D^2) samples are collected in Table I. For nonequivalent reflections that overlap in the powder pattern, the intensity $I(r)$ was split into the squared structure factors $F^2(h, k)$ with $h^2 + hk + k^2 = r$ according to their ratios in the electron diffraction pattern (Unwin and Henderson, 1975). The fourth column of Table I contains the Fourier difference coefficients ΔF_{Mea}. These values were used in the Fourier difference synthesis. The errors in ΔF_{Mea} were estimated by making three independent evaluations of the F_H and F_D data sets. As an error estimate for F_D and F_H we took the largest deviation from the mean in the three separate determinations of F_D and F_H. For the error in ΔF_{Mea}, indicated in parentheses in column four, we added the errors in F_D and F_H. The error due to the counting statistics was ~5% and always smaller than the overall errors. We note from Table I that the error in ΔF_{Mea}

TABLE I
STRUCTURE FACTORS, ΔF-VALUES, AND PHASES FOR SAMPLES LABELED WITH DEUTERATED (D) AND UNDEUTERATED (H) PITC

(h, k)	F_D^2	F_H^2	ΔF_{Mea}	ΔF_{RF}	ΔF_{Mod}	Phase radians
(1,0)	10,749.63	9,434.24	6.54 (0.5)	2.55	2.0	5.97
(1,1)	78,019.28	73,613.54	7.99 (0.6)	4.34	3.5	2.83
(2,0)	28,339.70	27,077.69	3.79 (0.7)	9.61	9.3	3.32
(2,1)	2,997.91	3,160.86	− 1.47 (0.9)	− 3.58	− 4.8	3.67
(1,2)	12,892.49	13,586.82	− 3.01 (1.7)	2.17	5.1	5.45
(2,2)	17,604.82	17,493.98	0.42 (1.2)	− 5.61	− 5.3	2.06
(3,1)	15,759.56	15,445.78	1.26 (1.5)	− 0.71	2.3	3.28
(1,3)	1,096.08	1,003.64	1.43 (1.0)	− 3.28	− 0.5	2.09
(4,0)	9,328.55	12,186.78	−13.81 (2.5)	−12.02	− 9.6	4.92
(3,2)	6,720.54	8,306.14	− 9.16 (2.9)	− 3.84	6.7	0.09
(2,3)	2,883.11	3,567.21	− 6.04 (1.7)	− 5.48	7.5	5.97
(4,1)	10,199.28	10,622.51	− 2.08 (1.0)	0.90	3.1	5.55
(1,4)	5,911.11	6,148.33	− 1.53 (1.5)	− 6.16	− 9.3	5.38
(5,0)	10,725.87	9,481.75	6.20 (1.5)	10.07	13.7	6.02
(4,2)	1,461.86	1,894.64	− 5.30 (1.0)	− 6.93	− 2.5	1.80
(2,4)	12,795.95	16,589.56	−15.68 (2.5)	− 4.78	− 3.0	4.19
(5,1)	380.87	359.86	0.55 (0.5)	2.99	5.4	0.49
(1,5)	5,386.03	5,082.74	2.10 (2.0)	0.62	4.7	4.68
(4,3)	24,806.49	28,978.47	−12.73 (3.0)	− 5.13	− 2.3	2.18
(3,4)	9,520.72	11,124.56	− 7.90 (2.2)	− 8.48	−12.3	2.83
(5,2)	19,036.07	13,092.19	23.55 (7.5)	11.23	15.2	2.27
(2,5)	3,124.03	2,148.90	9.53 (3.0)	10.00	10.8	4.75

$\Delta F = F_D - F_H$. ΔF_{Mea}, ΔF_{RF}, and ΔF_{Mod} are the changes in structure factors obtained by measurement, refinement, and model calculation, respectively. The estimated errors in ΔF_{Mea} are indicated in parentheses.

is in six cases larger than ΔF_{Mea} itself. All of these reflections have small ΔF values, however, and contribute little in the Fourier synthesis. The last column of Table I contains the phase information that was taken over from the electron diffraction work (Unwin and Henderson, 1975; Hayward and Stroud, 1981). The two approximations made, use of the phases and structure factor ratios from electron diffraction, have recently been discussed in detail (Plöhn and Büldt, 1985). Model calculations showed that at the present resolution these approximations, in the framework of the Fourier difference approach, lead to the correct result for the position of the label provided that the difference in scattering length between undeuterated and deuterated label is small (Plöhn and Büldt, 1985). This condition is satisfied in the present case. The native projected structure is shown in Fig. 6, based on all reflections up to and including (5,2). The last well resolved reflection was (7,0). Since no differences in intensity beyond (5,2) were observed, however, both the native and the Fourier difference map were calculated by summing the contributions up to and including (5,2). This corresponds to a resolution of 8.7 Å. For clarity only the ten positive contour lines are shown ranging in steps of 5% from 50 to 95% of the density. Using the ΔF_{Mea} values tabulated in Table I the Fourier difference map for the location of PITC was calculated. The result is shown in Fig. 5 *a*. For clarity only the 6 positive contour lines are shown, ranging in steps of 17% from 0 (not shown) to 100% of the positive difference density. The map has a single well localized maximum that is twice as high as the next highest feature.

The position and occupancy of the label site was further refined by using a standard crystallographic program for the refinement of heavy atom sites (Dickerson et al., 1968). In the procedure the label is assumed to be a point, which is a good approximation at this resolution for the five deuterons in the ring of PITC if it is completely immobilized in the structure. The point label is moved around and the occupancy is varied until a minimum is found in the "lack of closure" summed over all reflections:

$$\sum_{h,k}(|F_D(h,k)| - |F_H(h,k) + F_L(h,k)|)^2.$$

$|F_D|$ and $|F_H|$ are the observed structure factors for the samples labeled with deuterated and undeuterated PITC. F_L is the calculated structure factor contribution from the label, i.e., the replacement of five protons by five deuterons. The coordinates obtained in the Fourier difference procedure (Fig. 5 *a*) were used as starting values. The coordinates are expressed in relative cell units (see Fig. 5 *a*). x is the horizontal coordinate, y the oblique coordinate. As initial value for the position of PITC we used $x = -0.184$, $y = 0.187$. Progress in the minimization was measured using an R-factor, defined as the ratio of the sum of the squares of the "lack of closure"-residuals, divided by the sum of the squares of the observed differences in structure factors (ΔF_{Mea}):

$$R = \frac{\sum_{h,k}(|F_D(h,k)| - |F_H(h,k) + F_L(h,k)|)^2}{\sum_{h,k}(|F_D(h,k)| - |F_H(h,k)|)^2}.$$

At the end of the refinement the R factor had a value of 0.32 and the final label coordinates were $x = -0.181$, $y = 0.183$. We conclude that the refinement has changed the label position in only a very minor way. Since in this procedure the contributions of the label are added vectorially to the structure factors of the undeuterated protein, the approximation made in the Fourier difference synthe-

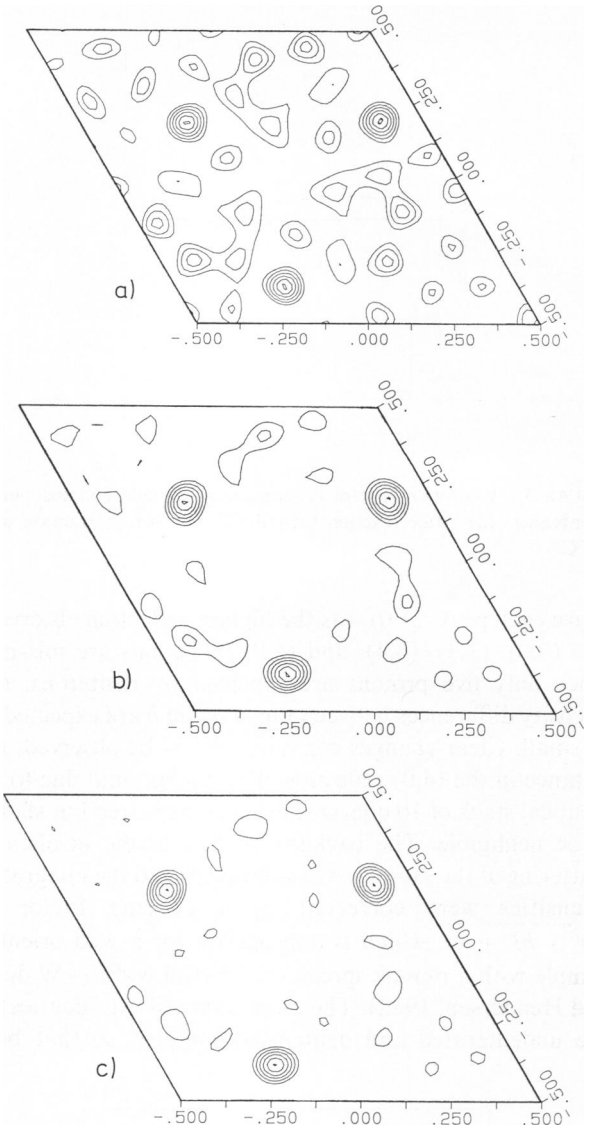

FIGURE 5 Fourier difference maps for the location of PITC. (*a*) Fourier difference map. (*b*) "Best" Fourier difference map, after refinement in reciprocal space. (*c*) Fourier difference map based on the model calculation. Only positive contours are shown.

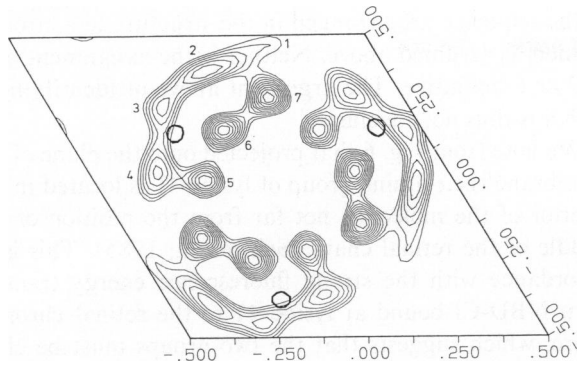

FIGURE 6 Projected density of the purple membrane as determined from the neutron diffraction intensities at 8.7 Å resolution. Negative contours have been omitted. The side of the hexagonal unit cell corresponds to 63 Å. Superimposed on the density is the 83% contour line from the Fourier difference map of Fig. 5 *b* for the position of PITC.

sis, namely the use of the same phases for both the undeuterated (F_H) and deuterated (F_D) structure factors is not made here. For the same reason the ratios of the intensities of the nonequivalent (h, k) and (k, h) reflections are no longer the same for the F_H and F_D structure factor sets after refinement. The unjustifiable assumption made in the Fourier difference approach, that this ratio remains the same after labeling, is abandoned in the refinement. By relaxing these two constraints a lower R value and a correspondingly cleaner Fourier difference map are obtained. Fig. 5 *b* is a "best" Fourier difference map in which the refined F_D values were used rather than the measured F_D values. Note that the label peak is now three times as high as the next highest feature. The refined ΔF values are listed in column 5 of Table I. Comparing ΔF_{Mea} with ΔF_{RF} we observe that refinement leads to a change in sign of five of the 22 ΔF values. Of these five reflections three have such small ΔF values that the errors are larger or of the order of the ΔF values themselves. The other two have also small ΔF values. Since these five reflections with small difference coefficients do not contribute much to the Fourier sum, it is not surprising that changing their sign, keeping their magnitude small, does not make a major difference in the corresponding map. In this connection we point out the well-known result that the Fourier difference synthesis is largely determined by the phases rather than by the amplitudes of those reflections that show major intensity changes. Setting all the small ΔF values equal to zero, replacing the remaining $|\Delta F|$ values by one and taking the signs obtained in the refinement, the resulting Fourier difference map is essentially the same as in Fig. 5 *a*. A double difference Fourier map of the difference between the observed and calculated F_D values shows only noise scattered throughout the unit cell indicating that the refinement converged to the correct solution.

It remains to be shown that the amplitude of the difference density observed in Fig. 5 *a* corresponds to that expected for the replacement of five protons by five deuterons. For this purpose model calculations were performed as described recently (Plöhn and Büldt, 1985). The map was put on an absolute scale in the following way. The neutron structure factors for the undeuterated sample were transformed into a density map on a 60 × 60 grid of points for the unit cell using the EM phases. The total scattering length of an average helix was determined by integration over the appropriate region in space. The correct scattering density for the label on this scale was determined by multiplying this average helical scattering length by the ratio of the calculated scattering length of the label (five deuterons minus five protons, 52.05 Fermi) and the calculated average scattering length of one helix (567 Fermi). This extra density was added to the density of the undeuterated sample at the point (−0.181, 0.183) determined in the refinement procedure. By transforming this density a set of predicted structure factors for the deuterated sample was obtained. The predicted Fourier difference coefficients ΔF_{Mod} (Table I, column 6) are in very good agreement with the coefficients ΔF_{RF} from the refinement procedure. The agreement with the experimentally observed ΔF_{Mea} values is also surprisingly good. There are only four changes in sign, occurring for reflections with relatively small difference coefficients. This result shows that the Fourier difference map of Fig. 5 *a* has indeed the appropriate amplitude expected for the label. To show this graphically, rather than through the agreement between columns 4 and 6 of Table I, we reproduce in Fig. 5 *c* the Fourier difference map with the coefficients ΔF_{Mod}. The agreement with Fig. 5, *a* and *b* is excellent.

In both the refinement and model calculations the label density was placed at the single site corresponding to the maximum of Fig. 5 *a*. We note from Fig. 5, *b* and *c* that in both cases a difference density is predicted which includes secondary maxima at exactly the same positions as observed in the Fourier difference map (Fig. 5 *a*). We may conclude therefore that these subsidiary maxima do not correspond to true label density (such as secondary PITC binding sites), but are rather due to cut-off and phase errors as well as intrinsic errors in the Fourier difference method.

DISCUSSION

This is the first report in which a chemically modified amino acid was located in the structure of a membrane protein by means of neutron diffraction. The results of this study moreover demonstrate that a label containing as few as five deuterons can be detected. The change in scattering length due to the replacement of five hydrogens by five deuteriums corresponds to about one tenth of the scattering length of an average helix. Although the label is thus not very weak, it contains nevertheless only half as many deuterons as the weakest label used so far (Seiff et al., 1985). The refinement and model calculations were integral parts of the evidence showing that the peak observed in the difference density corresponds to the label.

The labeling reaction was performed as described in the published procedure (Sigrist et al., 1984). These authors showed that the amount of bound label per bacteriorhodopsin saturates at a value close to one at a total label to bacteriorhodopsin ratio of 1,000:1 (Sigrist et al., 1981). The binding curve is a simple hyperbola and shows no evidence for secondary binding sites (Sigrist et al., 1981). The related labels 4-*N*,*N*'-dimethylamino-azobenzene-4'-isothiocyanate and 7-chloro-4-nitrobenz-2-oxa-1,3-diazole (NBD-Cl) were also shown to react exclusively at lysine 41 (Sigrist et al., 1984; Allegrini et al., 1983). Taken together these three labeling experiments indicate the existence of a unique ϵ-amino group at lysine 41. From a number of experiments it was furthermore concluded that the modification at lysine 41 occurs in a hydrophobic membrane domain (Sigrist et al., 1984; Allegrini et al., 1983). This is in accordance with our observation based on time-dependent and steady-state fluorescence depolarization that the fluorescent label NBD-Cl bound at lysine 41 is completely immobilized (Rehorek, Otto, Sigrist, and Heyn, unpublished observations). A small label of the size of NBD-Cl is expected to execute rapid rotations on the fluorescence time scale. The well-defined maximum observed in the Fourier difference map of Fig. 5 *a* is thus consistent with the idea of an immobilized label in a hydrophobic membrane environment. The accuracy with which the mean position of the label is determined is much higher than half the 8.7 Å resolution and is estimated to be of the order of 1 Å (Plöhn and Büldt, 1985).

Sample preparation appears to be the key to successful neutron diffraction work on biological membranes and a major part of our efforts was directed towards the goal of preparing identical deuterated and undeuterated samples. By using deuterated and undeuterated PITC the labeling was isomorphous.

Fig. 6 shows the position of the labeled PITC in the projected density of the purple membrane between helices 3 and 4. Although PITC is a small label, the length of the possibly fully extended lysine side chain introduces an intrinsic uncertainty in the assignment of helix *B* to which lysine 41 is attached. Taking these considerations into account, we can exclude helices 1 and 7 and probably also helix 2 as candidates for helix *B*. Helices 3, 4, 5, and 6 are clearly possibilities. There is no contradiction with previous neutron diffraction work that indicated that helix 3 should be identified with *F* (Trewhella et al., 1983). The assignment of (*D*, *E*, *F*, *G*, *A*, *B*, *C*) to (1, 2, 3, 4, 5, 6, 7) for instance would be consistent with both experiments. In our previous work with deuterated retinal (Seiff et al., 1985), we showed that helices 2 and 6 are candidates for helix *G*. Assuming a cyclical arrangement of the helices around the perimeter of the molecule, two assignments for (1, 2, 3, 4, 5, 6, 7) are consistent with both our present and previous work: (*F*, *G*, *A*, *B*, *C*, *D*, *E*) and (*E*, *D*, *C*, *B*, *A*, *G*, *F*). In both models helix *B* is identical with helix 4. There is, however, at present no compelling evidence that the helices of the sequence are arranged in the structure in a circular fashion as assumed above. Neither is the assignment of *G* to 2 or 6 definitive. The argument above of identifying *B* with 4 is thus not conclusive.

We note from Fig. 6 that projected onto the plane of the membrane the ϵ-amino group of lysine 41 is located in the interior of the molecule, not far from the position of the middle of the retinal chain (Seiff et al., 1985). This is in accordance with the strong fluorescence energy transfer from NBD-Cl bound at lysine 41 to the retinal chromophore, which suggests that the two groups must be close together (Rehorek, Otto, Sigrist, and Heyn, unpublished observations). This proximity is of considerable interest in connection with the recent report that after reduction in the dark 45% of the retinal is found to be linked to lysine 41 (Wolber and Stoeckenius, 1984). This retinal migration may well be facilitated by the proximity of lysine 41 and the retinal chromophore.

In conclusion we expect that further application of the chemical modification approach introduced here will lead to a complete solution of the helix assignment problem.

We thank R. Henderson and R. Stroud for providing us with the phases and structure factor ratios from their electron diffraction work. We are grateful to G. Büldt and H.-J. Plöhn for letting us use their model calculation program before publication; to J. Finer-Moore for help with the refinement calculations; to A. Fahr for continuous support with programming and computer systems; to H. Sigrist for his advice concerning the labeling procedure; and to the staff of the D-16 diffractometer of the Institute Laue-Langevin (Grenoble) for their support.

This work was supported by grant 03 B72C019 of the Bundesministerium für Forschung und Technologie.

Received for publication 10 December 1985 and in final form 20 May 1986.

REFERENCES

Agard, D. A., and R. M. Stroud. 1982. Linking regions between helices in bacteriorhodopsin revealed. *Biophys. J.* 37:589–602.

Allegrini, P. R., H. Sigrist, J. Schaller, and P. Zahler. 1983. Site-directed fluorogenic modification of bacteriorhodopsin by 7-chloro-4-nitrobenz-2-oxa-1,3-diazole. *Eur. J. Biochem.* 132:603–608.

Blundell, T. L., and L. N. Johnson. 1976. Protein Crystallography. Academic Press, Inc., New York. 404 pp.

Dickerson, R. E., J. E. Weinzierl, and R. A. Palmer. 1968. A least-squares refinement method for isomorphous replacement. *Acta Crystallogr. Sect. B Struct. Crystallogr. Cryst. Chem.* B24:997–1003.

Engelman, D. M., and G. Zaccai. 1980. Bacteriorhodopsin is an inside-out protein. *Proc. Natl. Acad. Sci. USA.* 77:5894–5898.

Engelman, D. M., R. Henderson, A. D. McLachlan, and B. A. Wallace. 1980. Path of the polypeptide in bacteriorhodopsin. *Proc. Natl. Acad. Sci. USA.* 77:2023–2027.

Gattermann, L., and H. Wieland. 1982. Die Praxis des organischen Chemikers. Walter de Gruyter, Berlin. 527 pp.

Hayward, S. B., and R. M. Stroud. 1981. Projected structure of purple membrane determined to 3.7 Å resolution by low temperature electron microscopy. *J. Mol. Biol.* 151:491–517.

Henderson, R. 1975. The structure of the purple membrane from *Halobacterium halobium*: analysis of the x-ray diffraction pattern. *J. Mol. Biol.* 93:123–138.

Henderson, R., and P. N. T. Unwin. 1975. Three-dimensional model of

purple membrane obtained by electron microscopy. *Nature* (*Lond.*). 257:28–32.

Jubb, J. S., D. L. Worcester, H. L. Crespi, and G. Zaccai. 1984. Retinal location in purple membrane of *Halobacterium halobium*: a neutron diffraction study of membranes labeled in vivo with deuterated retinal. *EMBO J.* 3:1455–1461.

Katre, N. V., J. Finer-Moore, R. M. Stroud, and S. B. Hayward. 1984. Location of an extrinsic label in the primary and tertiary structure of bacteriorhodopsin. *Biophys. J.* 46:195–204.

Khorana, H. G., G. E. Gerber, W. C. Herlihy, C. P. Gray, R. J. Anderegg, K. Nihei, and K. Biemann. 1979. Amino acid sequence of bacteriorhodopsin. *Proc. Natl. Acad. Sci. USA.* 76:5046–5050.

Oesterhelt, D., and W. Stoeckenius. 1974. Isolation of *Halobacterium halobium* and its fractionation into red and purple membrane. *Methods Enzymol.* 31:667–678.

Ovchinnikov, Yu. A., N. G. Abdulaev, M. Yu. Feigina, A. V. Kiselev, and N. A. Lobanov. 1979. The structural basis of the functioning of bacteriorhodopsin: an overview. *FEBS* (*Fed. Eur. Biochem. Soc.*) *Lett.* 100:219–224.

Plöhn, H.-J., and G. Büldt. 1985. The use of label techniques to determine membrane protein structure by diffraction. *J. Appl. Cryst.* In press.

Seiff, F., I. Wallat, P. Ermann, and M. P. Heyn. 1985. A neutron diffraction study on the location of the polyene chain of retinal in bacteriorhodopsin. *Proc. Natl. Acad. Sci. USA.* 82:3227–3231.

Sigrist, H., P. R. Allegrini, R. J. Strasser, and P. Zahler. 1981. Chemical modification of bacteriorhodopsin by phenylisothiocyanate: effect on the photocycle. *In* Proceedings in Life Sciences: The Blue Light Syndrome. H. Senger, editor. Springer-Verlag, Berlin. 30–37.

Sigrist, H., P. R. Allegrini, K. Stauffer, J. Schaller, N. G. Abdulaev, E. E. Rickli, and P. Zahler. 1984. Group-directed modification of bacteriorhodopsin by arylisothiocyanates. *J. Mol. Biol.* 173:93–108.

Stoeckenius, W., and R. A. Bogomolni. 1982. Bacteriorhodopsin and related pigments of halobacteria. *Annu. Rev. Biochem.* 52:587–616.

Trewhella, J., S. Anderson, R. Fox, E. Gogol, S. Khan, D. M. Engelman, and G. Zaccai. 1983. Assignment of segments of the bacteriorhodopsin sequence to positions in the structural map. *Biophys. J.* 42:233–241.

Unwin, P. N. T., and R. Henderson. 1975. Molecular structure determination by electron microscopy of unstained crystalline specimens. *J. Mol. Biol.* 94:425–440.

Wallace, B. A., and R. Henderson. 1982. Location of the carboxyl terminus of bacteriorhodopsin in purple membrane. *Biophys. J.* 39:233–239.

Wolber, P. K., and W. Stoeckenius. 1984. Retinal migration during dark reduction of bacteriorhodopsin. *Proc. Natl. Acad. Sci. USA.* 81:2303–2307.